Effect of Deposition Conditions to Mechanical and Tribological Properties of TiB_2 Based Nanostructured Coatings

N. Vattanaprateep* and N. Panich

Faculty of Engineering, Rajapark Institute, Bangkok, Thailand
*Corresponding Author: Tel. (02) 8870676, E-mail: nuntapolv@yahoo.com

ABSTRACT

In this work, fabrication and development of TiB_2-based nanostructured coatings was investigated in the present work. By varying the deposition conditions such as sputter-target power density, substrate temperature, deposition time, substrate-to-target distance, substrate biasing and substrate sputter cleaning, the relationship between the sputtered structure, properties and sputtering conditions were established. The experimental results showed that the target-to-substrate distance played a major role in the coating structure and properties. Sputter cleaning of substrate helped to improve TiB_2 coating hardness and adhesion. The deposition process could be controlled to produce a TiB_2 coating with both high hardness and good adhesion strength. This was achieved by introducing substrate sputter-cleaning and then biasing for the early stage of deposition, followed by deposition without biasing.

Keywords: TiB_2-based nanostructured coating, Nanoindentation, XRD, SEM, FESEM, Hardness, Modulus.

1. Introduction

Generally speaking nano-structured materials demonstrate excellent mechanical properties such as extraordinarily high hardness, tribological performance and yield strength. These uncommon properties may provide great potentials for the application of this new class of materials in many fields, including mechanical, automobile, aerospace and microelectronic engineering [1-3]. Increasing applications have been found for thin, hard, wear resistant (ceramic) coatings in metal cutting and metal forming tools. The invention of low temperature (below 500 ^oC) physical vapour deposition (PVD) processes such as magnetron sputtering has made possible the deposition of various hard and wear resistant coatings onto commonly used tool steels. When applied properly, protective coatings on cutting tools and other tribological components can extend component lifetimes. It is usually desirable to have coating with high hardness and low internal stress. Protective coatings with high hardness provide better wear resistance of coated tool steel against abrasion at high contact pressures [4].

Among many materials of interest, titanium diboride (TiB_2) has notably been chosen. TiB_2 possesses many interesting physical, mechanical and chemical properties, such as high hardness, high melting point, good chemical stability and good thermal and electrical conductivity. There have been increasing interests in fabrication of this material in thin film and coating forms for many potential applications, for example to reduce wear and corrosion in engineering components and particularly in material processing tools and dies [5-6]. Although TiB_2 coatings

have been widely studied by many researchers, their real applications have been very limited. The existing problem of TiB_2 coating is that its adhesion is poor for the coating-substrate system.

In the present investigation, attempts have been made to fabricate TiB_2-based nanostructured engineering coatings on high speed tool steel substrate under various parameters such as sputter-target power density, substrate temperature, deposition time, substrate-to-target distance, substrate biasing and substrate sputter cleaning. The characterization of their structures and mechanical properties for the resultant coatings has been carried out.

2. Experimental Details

In this study, high speed steel (HSS), SECO WKE45 (Sweden), in fully hardened and tempered condition was chosen as substrates. The specimen surface was manually ground and polished. The HSS substrates were then ultrasonically cleaned with acetone and ethanol before charging into the deposition chamber. A planar magnetron sputtering system supplied by the Coaxial Company (UK) was used for depositions. The system consists of a cylindrical chamber with three 3-inch water cooled target holders tilted at approximately 30 degree with respect to the normal of the horizontal substrate holder, which can be heated by graphite heating elements. The substrates can be stationary and rotated and the substrate-target distance can be adjusted from 60 mm to 100 mm for TiB_2 and Ti targets. All the experiments were conducted at a constant working pressure of 0.65 Pa and at a total gas flow rate (Ar) of 20 sccm. The substrate temperature can be changed from room temperature (RT) until 400 ºC. A RF power biased to the substrate was used to sputter clean the substrate surface. Both DC and RF sputtering were used in this work by using DC power for the Ti target and RF power for the TiB_2 target. The DC and RF power employed in this study was varied from 200-400 W. The details of deposition are summarized in Table 1.

The phase identification of the resultant coatings was examined by Shimadzu X-ray diffractometer with Cu-K_α radiation. The fractured cross-sections of the coatings were imaged using a field emission scanning electron microscope (FESEM), Jeol JSM 6340F. The coating thickness was measured by making a ball-crater on the coating surface using the Calotest machine available at Nanoshield Co. Ltd. manufactured by CSM, Switzerland. The roughness of surfaces was imaged using an atomic force microscopy (AFM).

Nanoindentation test was performed with a Berkovich diamond indenter. Experiments were performed at a constant loading and unloading rate of 0.05 mN/s. In order to assess the intrinsic mechanical properties of the coatings i.e. hardness and modulus, all specimens were tested at 50 nm penetration depth to avoid any possible effect from the substrate during the indentation process. The unloading curves were used to derive the hardness and reduced modulus values by the analytical technique developed by Oliver and Pharr [7]. The reported hardness and modulus values are the average of 10 measurements.

The microscratch test was performed using the single-pass scratch mode with a Rockwell diamond indenter topped as a conical with spherical end form of 25 μm in radius. The scanned length was scratched by applying a linearly increasing load at 5 mN/s after prescanning the initial 50 μm distance under a small initial load of 0.25 mN. During scratching, the friction force on the indenter and the surface profile along the full length of the scratched track were measured continually, such that a friction force versus scratching distance (or load) curve was obtained. The critical load for coating failure (Lc), commonly used to measure of the coating-substrate adhesion strength, was determined by the sudden change in friction force.

3. Results and Discussion

Two sets of experiments were first conducted to study the effect of various parameters on the structure and properties of single layer TiB_2 coatings with a Ti interlayer (Figure 1). The purpose of depositing a thin Ti interfacial layer by sputtering a pure Ti target for a few minutes is to increase the adhesion between HSS substrate and TiB_2 coating. The first set was performed without substrate cleaning and biasing with the purpose to determine the best combination of other parameters in terms of structure and properties. The second set employed the optimized condition and introduced substrate sputter cleaning and biasing during deposition to further enhance the structure and properties characteristics.

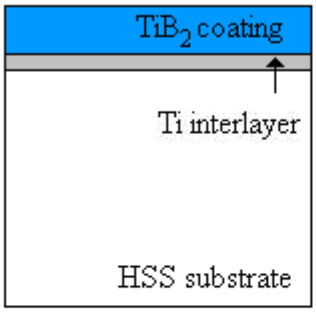

Figure 1: Schematic of single layer TiB_2 coating on HSS with a Ti interlayer.

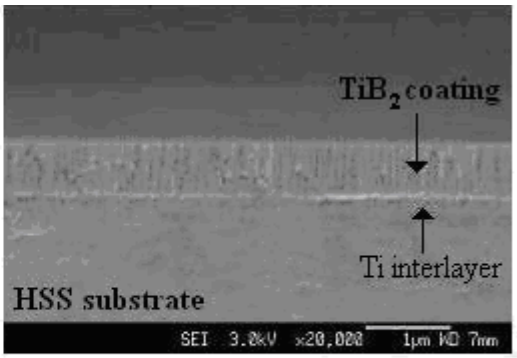

Figure 2: FESEM image of fractured cross-section of samples S1-6.

3.1 Structural Characterization

Table 1 summarizes the deposition conditions and Table 2 summarizes the properties of resultant coating samples. Typical fractured cross-sectional morphology of selected coatings in this Set is given in Figure 2, which shows the columnar growth of the TiB_2 coatings and a thin Ti interlayer. Details of structural and properties features are given below.

Table 1: Summary of deposition conditions for TiB_2 coatings.

Sample	Substrate Temperature (°C)	Ti Power/Time	TiB_2 Power/Time	TiB_2 Target/ Substrate Distance
Set1-1	RT	150 W/ 5 min	150 W/ 2 hours	100 mm
S1-2	100	150 W/ 5 min	150 W/ 2 hours	100 mm
S1-3	200	150 W/ 5 min	150 W/ 2 hours	100 mm
S1-4	300	150 W/ 5 min	150 W/ 2 hours	100 mm
S1-5	300	300 W/ 5 min	300 W/ 2 hours	100 mm
S1-6	400	350 W/ 20 min	350 W/ 3 hours	100 mm
S1-7	400	200 W/ 10 min	200 W/ 3 hours	60 mm

Table 2: Summary of the resultant coating properties.

Material	Coating Thickness (μm)		TiB_2	Hardness	Elastic Modulus	Critical Load (mN)
	Ti	TiB_2	Texture	(GPa)	(GPa)	
S1-1	0.05	0.35	(101)	8.2	166.6	20.8
S1-2	0.05	0.35	(101)	10.0	184.1	21.1
S1-3	0.05	0.35	(101)	8.1	171.7	26.5
S1-4	0.05	0.40	(101)	7.8	171.6	10.2
S1-5	0.10	0.65	(101)	11.1	189.5	18.1
S1-6	0.25	0.75	(101), (001)	17.1	208.5	65.0
S1-7	0.15	0.55	(001)	28.4	307.2	74.5

X-ray diffraction analysis shows that all the TiB_2 coatings produced with low TiB_2 target power (samples S1-1 to S1-4) exhibit a broad diffraction peak corresponding to the TiB_2 phase irrespective of deposition temperature (Figure 3). Small peaks of Ti were also found as expected which are from the Ti interlayer. The presence of a single peak suggests a fiber texture with preferred (101) orientation in the TiB_2 coatings.

From the literature, most of the TiB_2 coatings reported display the patterns of the hexagonal phase with a preferred (001) orientation [8-9] and the (001) oriented coatings yield the highest hardness [10]. The hexagonal TiB_2 phase in samples S1-1 to S1-4 did not demonstrate the preferred (001) orientation even with increased temperature to 300 ºC. It is noted that since the (001) plane has the highest packing factor, energetic adatom are required to create such an orientation [11]. With this in mind, further depositions were conducted by increasing the deposition power from 150 W to 300 W (sample S1-5). Unfortunately, this has little effect on the orientation of TiB_2 coating (Figure 3). Attempts were thus made to further increase the sputtering power to 350 W, substrate temperature to 400 °C and deposition time to 3 hours (sample S1-6). In this case, the (001) reflection appears in the diffraction pattern, indicating that the coating starts to orient in this direction. It thus appears that increasing sputtering power, substrate temperature and deposition time, favours the evolution of the (001) orientation.

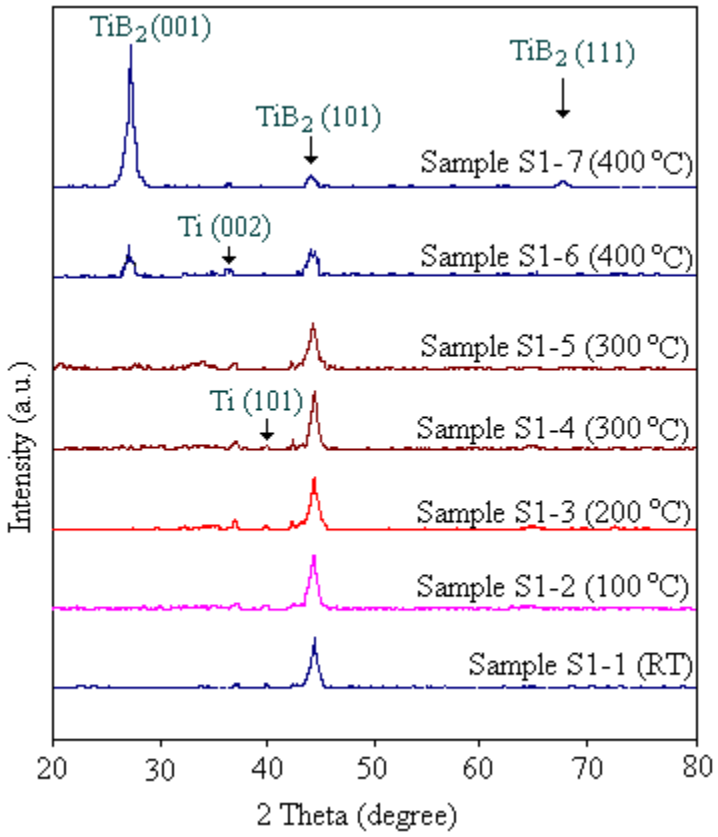

Figure 3: XRD patterns generated from single layer TiB_2 coatings with a Ti interlayer.

In order to enhance the development of the desired (001) orientations, another deposition was conducted by reducing the TiB_2-target-substrate distance from 100 mm to 60 mm (sample S1-7). The sputtering power was reduced to 200 W because it was found that the TiB_2 target cracked after several depositions at 300 W. The XRD result shown in Figure 3 reveals the development of a strong (001) texture in the coating.

3.2 Mechanical and Tribological Properties

(a) Nanoindentation Test

Although nanoindentation has been carried out at various indentation depths, due to the thin coating thickness (Table 2), the hardness and modulus values summarized in Table 2 were obtained from 50 nm depth, which is expected to minimize substrate effect. It can be seen that all the TiB_2 coatings with (101) orientations (samples S1-1 to S1-5) exhibit hardness and modulus values lower than those expected for bulk TiB_2 and those reported by other investigators [11-12]. This low hardness would be due to the poor orientation, small thickness and poor adhesion of the coating. Indeed, with increasing coating (001) orientation, the highest hardness of 28.4 GPa was obtained in sample S1-7, which is close to many reported values [13-14].

It is also worth to note the response of the coating to large indentation depth. Figure 4 shows the load-displacement curves of sample S1-6 produced at 300 nm depth. It is noted that pop-in event (arrow points at 1) occurs during loading, whilst pop-out event occurs during

unloading (arrow points at 2) of some indentations. These non-linear phenomena were observed commonly in the single layer TiB_2 coatings (samples S1-1 to S1-7), and is associated with the brittleness of the coating and poor coating/substrate adhesion, which lead to coating cracking or debonding during the indentation process.

In order to gain a better understanding of the indentation deformation and cracking behaviour, selected indents produced at large depth were examined by SEM, as shown in Figure 5 for sample S1-6. Figure 5 (a) shows an indent at 500 nm depth, from which it is clearly seen that the sink-in effect takes place. However, the coating is cracked if the indentation is made at 1,500 nm in depth (the coating thickness of sample S1-6 is only 950 nm) as shown in Figure 5 (b). This shows that the coating is such brittle that cannot carry a higher indentation load. Further study of imprinted nanoindentation at 700 nm is shown in Figure 5 (c) using AFM. This shows clearly for the indentation and calculate the true area for hardness calculation.

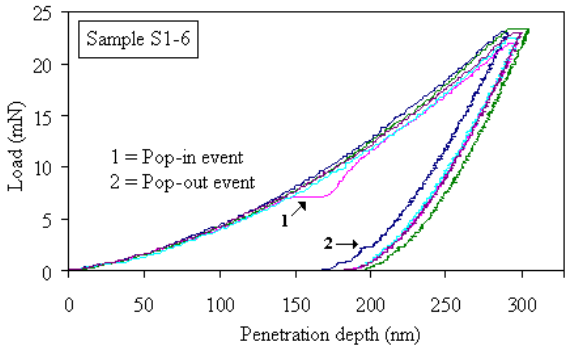

Figure 4: Load-displacement curves of sample S1-6.

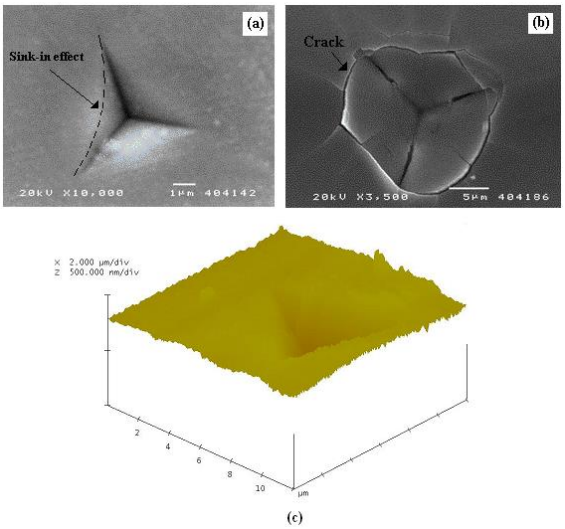

Figure 5: SEM images of sample S1-6 at indentation depth (a) 500 nm (b) 1,500 nm and (c) AFM image of imprinted nano-indentation at 700 nm.

(b) Microscratch Test

Coating adhesion was assessed using the microscratch adhesion test. The simplest method for evaluating the critical load for coating failure is to plot friction force vs load. Optical and

scanning electron microscopic (SEM) examinations were also used to confirm the results from the friction curve. The results are summarized in Table 2.

As expected, since samples S1-1 to S1-5 have a very thin coating thickness, cohesive failure could not be detected, and only adhesive failure could be found. The critical load, L_C, for adhesive failure of these coatings was found to be very low, in the range between 16 mN to 30 mN (Table 2). No correlation has been found between L_C and substrate temperature and sputtering power. Figure 6 shows typical scratch tracks measured by optical microscope (Figure 6 (a)) and AFM (Figure 6 (b)) which the mechanism of coating failure can be observed.

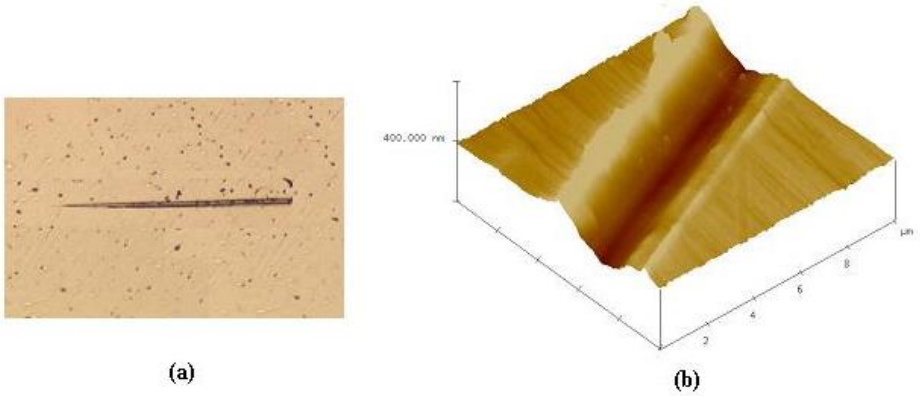

Figure 6: Microscratch tracks measured by optical microscope (a) and AFM (b).

From Table 2, it can be seen that the critical load was measured to be 65 mN in sample S1-6, which also showed a higher hardness. Sample S1-7 showed the highest L_C value of 74.5 mN, which also exhibits the highest hardness and strongest (001) orientation.

4. Summary

Based on the experiments, the main results are summarized as follow.

1. TiB_2 target rf power density does not have significant effect on TiB_2 coating structure and properties but increased power results in the cracking of the ceramic TiB_2 target. Thus, a low rf power of 200 W was used throughout this work.
2. Substrate temperature has a significant effect on coating structure and texture: high temperatures favour formation of dense, hard, (001) oriented and adherent coating.
3. Target-substrate distance has must be sufficiently short (< 70 mm) in order to produce high quality coatings. 60 mm distance was used for most depositions.
4. Sputter-cleaning of targets is beneficial in enhancing coating-substrate adhesion and coating hardness, but there exists an optimum sputter-cleaning time.
5. Substrate biasing is beneficial in enhancing coating-substrate adhesion, but tends to impair coating hardness, particularly when the biasing power is too high. It can be tailored to achieve best combination of hardness and adhesion.

5. Acknowledgements

Authors would like to thank you Rajapark Institute for financial support to this study.

References

[1] Samsonov, G.V., & Vinitskii, I.M. (1980). *Handbook of Refractory Compounds*. New York: IFI Plenum Data Company.

[2] Dempsey, E. (1963). Bonding in Refractory Hard Metals. *Philosophy Magazine*, 3, 86, 285-299.

[3] Friedel, J. (1969). *The Physics of Metals* ed. J.M. Ziman, Cambridge: Cambridge University Press.

[4] Matthes, B., Herr, W., Broszeit E., KloosG. Nürnberger, K. H., SchmoeckelF, Höhl, D., Stock, H.R., & Mayr, P. (1991). Tribological properties and wear behaviour of sputtered titanium-based hard coatings under sheet-metal-forming conditions. *Materials Science and Engineering* A, 140, 593-601.

[5] Ronald G. M. (2000). Material properties of titanium diboride. *Journal of Research of the National Institute of Standards and Technology*, 105, 709-720.

[6] Cutler, R. A. (1991). Engineering properties of borides. *Engineering Materials Handbook: Ceramic and Glasses*. ASM International, 4, 787-803.

[7] Oliver, W. C., & Pharr, G. M. (1992). An improved technique for determining hardness and elastic modulus using load and displacement sensing indentation experiments. *Journal of Materials Research*, 7, 1564-1583.

[8] Berger, M., Larsson, M., & Hogmark, S. (2000). Evaluation of magnetron-sputtered TiB_2 intended for tribological application. *Surface Coatings and Technology*, 124, 253-261.

[9] Berger, M., Karlsson, L., Larsson M., & Hogmark, S. (2001). Low stress TiB_2 coatings with improved tribological properties. *Thin Solid Films*, 401, 1-2, 179-186.

[10] Holleck, H. (1986). Material selection for hard coatings. *Journal of Vacuum Science and Technology* A, 4, 2661.

[11] Kelesoglu, E., & Mitterer, C. (1998). Structure and properties of TiB_2 based coatings prepared by unbalanced DC magnetron sputtering. *Surface Coatings and Technology*, 98, 1483-1489.

[12] Berger, M. (2002). Thick physical vapour deposition TiB_2 coatings. *Surface Engineering*, 18 (3), 219-223.

[13] Pfohl, C., Bulak, A., & Rie, K.-T. (2000). Development of titanium diboride coatings deposited by PACVD. *Surface Coatings and Technology*, 131, 141-146.

[14] Yang, Y., Zheng, Z., Wang, X., Liu, X., Han, J. G., & Yoon, J. S. (1996). Microstructure and tribology of TiB_2 and TiB_2/TiN double-layer coatings. *Surface Coatings and Technology*, 84, 404-408.